

## Molecular-dynamics simulations of methyl-radical deposition on diamond (100) surfaces

Dominic R. Alfonso

*Department of Chemistry and Condensed Matter and Surface Sciences Program,  
Ohio University, Athens, Ohio 45701-2979*

Sergio E. Ulloa

*Department of Physics and Astronomy and Condensed Matter and Surface Sciences Program,  
Ohio University, Athens, Ohio 45701-2979*

(Received 14 June 1993)

We have performed molecular-dynamics simulations using realistic many-body semiclassical potentials for hydrocarbon interactions to investigate the deposition dynamics of hyperthermal  $\text{CH}_3$  on diamond (100) surfaces. The adsorption probability was studied as a function of different incident radical and substrate conditions. Relevant energy exchange processes between incident molecules and the substrate were also analyzed. Three types of events were observed in the simulations: (i) adsorption events where  $\text{CH}_3$  bonds onto a surface radical "site," (ii) reflection events where  $\text{CH}_3$  backscatters to the gas phase, and (iii) surface-hydrogen knock-out events at high incident  $\text{CH}_3$  energy. The adsorption probability was found to be higher for normal incidence to the surface, and to increase for larger incident kinetic energies. The adsorption efficiency is not sensitive to surface H coverage except at lower  $\text{CH}_3$  energies. No chemisorption of the radical on a surface that is fully hydrogen terminated is observed, indicating that a radical site is needed for the  $\text{CH}_3$  to bind on the surface. Significant energy transfer through collision is observed.

### I. INTRODUCTION

Advances in the synthesis of diamond and diamond-like films and coatings at low temperature and pressure have fueled a great deal of interest in these materials. Various growth methods are used, such as chemical vapor deposition (CVD),<sup>1</sup> rf and dc plasma deposition,<sup>2</sup> laser plasma source technique,<sup>3</sup> mass separated ion-beam deposition,<sup>4</sup> and sputtering methods.<sup>5</sup> These techniques produce films with potential commercial applications, such as machine tools, optical coatings, and high temperature electronics.<sup>6,7</sup> It is of note that among the growth schemes mentioned, ion-beam deposition methods operate at a much lower substrate temperature. However, the beam energy values reported in the literature are clearly hyperthermal at 40–80 eV,<sup>2(d)</sup> 115–215 eV,<sup>4(c)</sup> or 100–500 eV.<sup>8</sup> The films grown show a mixture of  $sp^2$  and  $sp^3$  bonding as contrasted to crystalline diamond films which are purely  $sp^3$  coordinated.<sup>3</sup> Recent theoretical work relevant to the ion-beam deposition technique has appeared, as the authors investigate the stress distribution in the substrate caused by the impinging atoms and the actual structure of the growing film.<sup>8,9</sup>

Another proposed technique is low-energy molecular-beam deposition of diamond, which deposits hydrocarbon species at a much lower energy compared to ion-beam deposition.<sup>10</sup> The beam energies employed here are in the range 0.1–20 eV. Damage to the substrate by the impinging gas molecule is minimized and therefore this scheme shows promise for growing better quality films, as contrasted to the more energetic ion-beam methods. It is also possible that this would be a good approach for reducing defects in the growth process. The substrate can

be kept relatively cool during deposition while supplying the additional excitation required to grow high-quality material by specific interaction of the impinging species with the surface. Since the beam energy is hyperthermal, significant change in the adsorption dynamics from those of conventional deposition processes such as CVD is expected.

In this paper, we employ molecular-dynamics simulations to investigate the adsorption phenomena which may affect the low and intermediate energy molecular-beam deposition of diamond. Two dynamical properties are of particular interest: (i) a simple description of adsorption dynamics of the incident molecule including such factors as the sticking coefficient and the location of the adsorbed molecule, and (ii) scattering of substrate atoms. These quantities are relevant for a detailed description of the consequences of low energy molecular-beam growth. Indeed, the excess kinetic energy of the molecular beam must be accommodated by the substrate in order for the incoming particle to "stick." It is of particular interest, therefore, to look into the relevant energy exchange processes occurring between the incident molecule and the substrate.

In these simulations, we consider methyl radical ( $\text{CH}_3$ ) as the growth species and diamond (100) as the substrate. Various theoretical studies have suggested  $\text{CH}_3$  as an important precursor on the growing surface.<sup>11–13</sup> Molecular-dynamics simulations of hyperthermal deposition of  $\text{CH}_3$  on diamond (111) surfaces is also currently underway.<sup>14</sup> In addressing the role of various incident molecule and substrate conditions, we find that there is a general increase in the sticking coefficient of  $\text{CH}_3$  as the incident molecule becomes more energetic. The maxi-

imum sticking coefficient is observed when the incidence is normal to the surface, as one would expect on simple grounds. We find no significant change in the deposition dynamics for a substrate temperature range of 300–900 K. Moreover, we investigate the energy transfer processes that occur in the deposition events. We discover that chemisorption of the incident species on a surface radical site will take place if the excess kinetic energy of  $\text{CH}_3$  is carried away by the substrate lattice excitation. In what follows, the methodology, and then the results of the simulations, are presented and discussed.

## II. THEORETICAL METHODS

We employ an empirical many-body potential which realistically describes bonding in hydrocarbon systems and assumes the form<sup>15</sup>

$$U = \sum_i \sum_{j>i} [V_r(r_{ij}) - B_{ij}V_a(r_{ij})], \quad (1)$$

where  $V_r$  and  $V_a$  are terms which represent pair-repulsive and pair-attractive interactions, respectively, while  $B_{ij}$  is a many-body bond order term which depends on atomic coordinations and angles.<sup>16</sup> This potential is based on a Tersoff bond-order expression which contains terms that correct for overbinding of radicals and consider non-local effects.<sup>15,16</sup> The potential predicts that the  $(2 \times 1)$  reconstruction is energetically preferred for a clean surface in agreement with a first-principles calculation.<sup>15</sup> It also yields energetics and dimer bond lengths that agree with predictions from molecular mechanics calculations for the case when the dimer reconstructed (100) surface is hydrogen terminated.<sup>15</sup>

To model a (100) diamond surface, we utilize a slab of eight layers of carbon atoms having four atoms per layer, with the (100) face exposed reconstructed into a  $(2 \times 1)$  dimerized surface and terminated by hydrogen atoms. The bottom two layers are held rigid to their equilibrium position, representing a semi-infinite crystal, while the remaining layers were allowed to move with full dynamics. The substrate temperature is maintained by immersing the carbon atoms on the third, fourth, and fifth layer from the bottom in a thermostat employing the velocity scaling method of Berendsen *et al.*<sup>17</sup> Periodic boundary conditions were employed in the two directions parallel to the surface. A hydrogen atom was removed from the fully hydrogen terminated surface to model a 75% hydrogen covered surface, while a second hydrogen atom was removed from the other carbon belonging to the same dimer in order to model a surface which is 50% hydrogen covered. To evaluate whether our system is sufficiently large to model the deposition process, we ran several trajectories on a substrate that contains 24 carbon atoms per layer. We found no significant variation in the deposition dynamics of the radical on the larger substrate, suggesting that the smaller system is appropriate for these investigations.

The calculation is initiated by equilibrating the substrate to a desired temperature. A  $\text{CH}_3$  radical with incident center of mass energy  $E_i$  and incident angle  $\Theta_i$  is allowed to collide with the surface. All trajectories were

calculated with  $\text{CH}_3$  initially oriented at random Euler angles with respect to the surface. The initial position of the center of mass of the incident molecule is chosen from the random sets of coordinates in the plane of the surface and then backed from the surface such that the molecule experiences no initial interaction with the substrate. The trajectories of all the particles were determined by integrating the equations of motion according to the velocity form of the Verlet algorithm.<sup>18</sup> The integration proceeds until either the incoming molecule is adsorbed on the surface or is freely moving away from the substrate, beyond the range of interaction of all atoms still attached to the surface.  $\text{CH}_3$  is considered to be adsorbed when it bounces four times against the surface, as we observed empirically that this number is an approximate threshold for attachment. The typical time step employed in the simulations is 0.25–0.5 fs.

## III. RESULTS AND DISCUSSION

### A. Trapping and scattering of $\text{CH}_3$

Figure 1 summarizes the adsorption probabilities of  $\text{CH}_3$  for various conditions of the incident molecule and substrate. The substrate's temperature in these runs was maintained at  $T_s=300$  K. The calculation of adsorption probabilities is based on 150 collision events. We found that simulations with 150 trajectories randomly distributed across the surface unit cell gave acceptable statistics with errors of a few percent.

Figure 1 shows that the adsorption probability increases as the kinetic energy of the center of mass of the incident  $\text{CH}_3$  increases for the case of normal incidence to the surface ( $\Theta_i = 0$ ) and 75% of H coverage. Analysis of a video of the simulations showed that the chemical reaction associated with the adsorption event is the formation of a bond between the carbon in  $\text{CH}_3$  and a radical missing-hydrogen site on the surface. We performed similar calculations for the case where the sub-

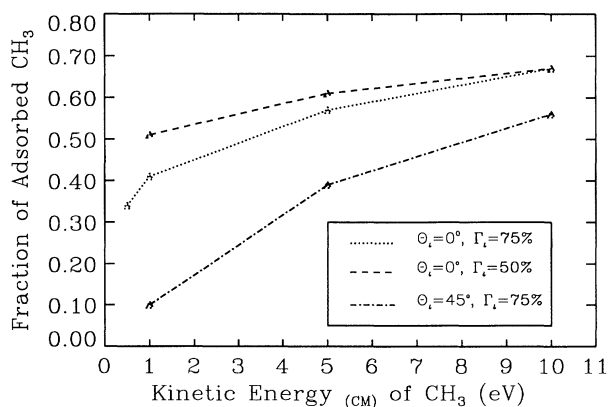


FIG. 1. The fraction of adsorbed events for  $\text{CH}_3$  incident on diamond (100) surface for various incidence and substrate conditions. Substrate temperature is held constant at 300 K.  $\Theta_i$  denotes the angle of incidence of  $\text{CH}_3$  with respect to the normal, and  $\Gamma_i$  the percent of hydrogen coverage of the surface.

strate is fully hydrogen terminated and we did not observe any adsorption event for this energy range. This result demonstrates that even for the rather broad range of energy we employed, adsorption events will not occur if radical sites are not present on the surface. Although this result was anticipated qualitatively, it is still somewhat surprising to see how strongly it is indeed verified. Formation of a bond between  $\text{CH}_3$  and the carbon belonging to the surface dimer pair is a very important reaction since subsequent abstraction of H from the adsorbed  $\text{CH}_3$  could promote  $\beta$ -scission<sup>13</sup> — a necessary condition for initial diamond growth on a diamond reconstructed (100) surface.

For runs which differ only in the H coverage of the surface, Fig. 1 shows a general increase in the fraction of  $\text{CH}_3$  adsorbed for lower H coverage. This is intuitively expected since a reconstructed diamond (100) surface with a lower hydrogen coverage offers more reactive sites per surface unit cell and less steric hindrance for the adsorption of the incoming gas molecule. Of course, analysis of the trajectories shows that  $\text{CH}_3$  binds equally to either carbon belonging to a surface dimer pair which is not initially hydrogen terminated. Notice also that the rise in adsorption probability becomes less pronounced as kinetic energy of the incident  $\text{CH}_3$  goes up. For the case where the energy of the incident molecule is initially 10 eV, our simulations showed no essential change in the adsorption efficiency of  $\text{CH}_3$  on both the 50% and the 75% coverage terminated surface. This result implies that the reactivity of the surface is likely the rate-limiting feature in the adsorption process at intermediate energies ( $\approx 1$ –5 eV). On the other hand, as  $\text{CH}_3$  becomes more energetic, the probability that it will be adsorbed on the surface is less sensitive to the availability of more reactive sites and steric hindrance on the surface — the high-energy molecule makes room by itself. At high energies, we notice events where the incident molecule displaces surface H atoms producing even H detachment (see below).

The effect of decreasing the angle of incidence to  $\Theta_i=45^\circ$  is to produce a substantial drop in the fraction of gas molecules adsorbed (see Fig. 1). This calculation was performed for a 75% hydrogen covered substrate. It would appear that the adsorption probability is linearly dependent on the normal velocity component of the center of mass of the incident molecule, although a precise dependence was not extracted from the data. Calculations were also performed to see whether the substrate temperature will affect deposition dynamics. The simulations did not indicate a significant change in the adsorption probabilities on varying the temperature over the range 300–900 K, as one would expect the hyperthermal incident molecule energies to dominate this process.

The nonreactive events observed are characterized by backscattering of the  $\text{CH}_3$  to the gas phase after it collides with the substrate. Moreover, we observed unexpected scattering events where the incident  $\text{CH}_3$  radical dislodges a surface H atom from its bonded configuration sending it to the gas phase. This event occurs when the molecule is incident with a normal energy above 1 eV, and is found to be more pronounced for a normal energy of 10 eV (the probability of H dislodging per col-

lision at this energy is 0.09 and 0.12 for a 50% and a 75% H covered surface, respectively). The surface hydrogen atom is in an exposed position with respect to the incoming molecule, as it is subjected to strong forces that can break its bond with the surface carbon, especially at higher collision energy. This abstraction process provides an indication that  $\text{CH}_3$  can also play a role in providing radical sites on the surface aside from being a growth species at higher incident energy conditions.

## B. Energy loss rate

We have examined the relevant energy exchange processes taking place as  $\text{CH}_3$  collides with the surface. For several trajectories, kinetic energies and the height of the center of mass of the molecule were monitored throughout the simulation until 2.5 ps elapsed. All trajectories leading to an adsorption event share features similar to Fig. 2. During the adsorption process, the gas molecule loses energy at each bounce on the surface. A  $\text{CH}_3$  undergoing multiple bounces against the surface eventually loses almost all of its energy and thermalizes to the substrate, typically within a picosecond. It is evident from Figs. 2 and 3 how quickly an incident  $\text{CH}_3$  loses memory of its initial condition. Notice that after  $t \geq 10^3$  fs,  $\text{CH}_3$  has basically thermalized with the substrate, keeping a distance  $\approx 0.5$  Å from the surface and  $\langle \text{KE}_{\text{CM}} \rangle \approx kT$ . Notice that the thermalization time is only a few tens of times the characteristic diamond phonon period ( $\nu^{-1} \approx 1/30$  THz  $\approx 30$  fs), which indicates that the substrate is extremely efficient in dissipating the additional energy at the surface without suffering any damage (see below).

Figure 3 exhibits a typical energy vs time profile for a  $\text{CH}_3$  backscattered from the surface. The gas molecule bounced on the surface once transferring a significant amount of energy ( $\approx 80$ ) to the substrate and to internal potential energy, and leaving it with a much reduced kinetic energy of 1.4 eV. Further ahead, the molecule decreases its interaction with the substrate after the initial bounce at  $t \approx 60$  fs and slowly moves away from the sur-

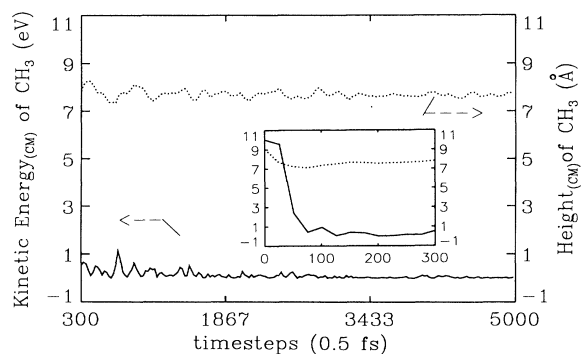


FIG. 2. Time evolution of the kinetic energy and height of the center of mass of  $\text{CH}_3$  for an adsorption event. Inset shows the first 150 fs, while the main figure shows up to 2.5 ps. The molecule was incident normally at 10 eV on the surface. The height of the top surface is  $\approx 8$  Å.

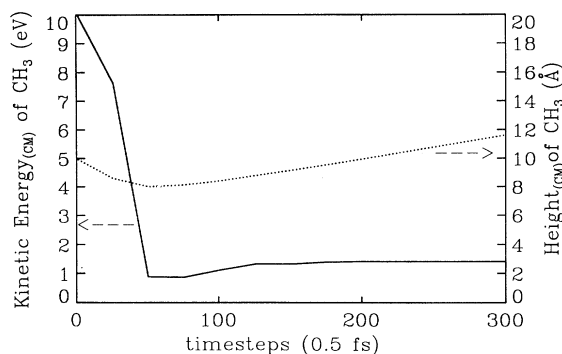


FIG. 3. Time evolution of the kinetic energy and height of the center of mass of  $\text{CH}_3$  for a *backscattering* event where the molecule is incident normally on the surface at 10 eV. The height of the top surface is  $\approx 8$  Å.

face afterwards after transferring over 70% of its energy.

In order to explore the state of the sample surface and possible damage after each collision, we have calculated average displacements of the carbon atoms in the substrate (displacement is defined as the net separation of each carbon atom from its equilibrium position before collision). We show results for  $\text{CH}_3$  incident with a normal kinetic energy of 1 and 10 eV and subsequently adsorbed on a substrate with 75% H coverage and maintained at 300 K. Figure 4 shows that the energy process is governed by excitation of surface phonons and subsequent transfer of energy from one atomic layer to another. This figure shows atomic displacements of the surface carbon atoms after 2.5 ps, when the incident molecule has already thermalized. Notice that disruption of the surface is much larger for the event in the top panel of Fig. 4, since total energy transfer is larger. The top panel also shows atomic displacements after the first “bounce” in Fig. 2, at approximately 40 fs, to show the extent of the initial impact. Despite the rather large initial displacements, the system relaxes back after thermalization, as we found no evidence of substrate damage even at these high energies. This is confirmed by visual inspection of the resulting structures. This result is encouraging for the possible realization of low energy molecular-beam growth, where incident energy is expected to be typically in the range studied here. The lack of induced damage, if at least in these low flux conditions, is promising of good quality samples if growth is indeed nucleated.

#### IV. CONCLUSIONS

The molecular-dynamics simulations described in this paper represent the individual deposition process of  $\text{CH}_3$  radicals on reconstructed diamond (100) surfaces. The predicted adsorption efficiency depends monotonically on the incident normal kinetic energy, as the energy of the molecule is increased until 10 eV. We did not observe significant changes in the deposition dynamics when the

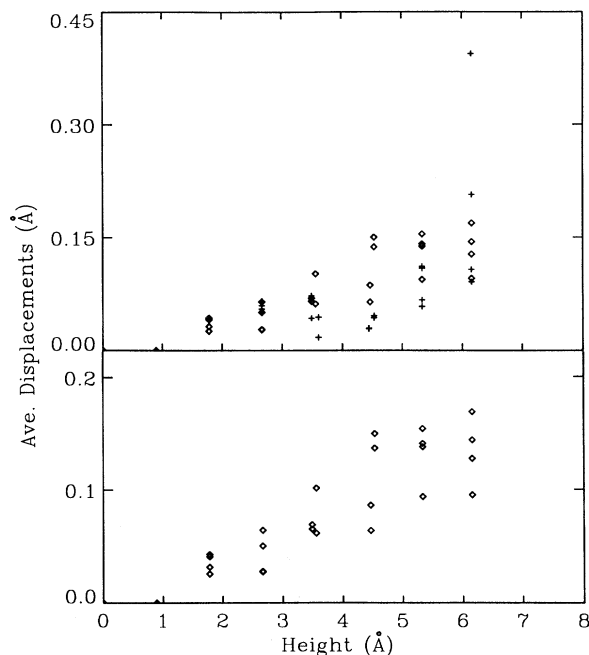


FIG. 4. Displacements of the carbon atoms of the substrate from their initial positions as a function of their depth on the substrate after 2.5 ps for an adsorption event. Top panel: initial normal-incidence kinetic energy is 10 eV; bottom panel: initial kinetic energy is 1 eV. Each diamond represents a single atom. Crosses in the top panel show displacements right after the initial closest approach, at  $\approx 40$  fs.

substrate temperature is increased up to 900 K. Very energetic  $\text{CH}_3$  molecules at about 10 eV are not sensitive to the number of available radical sites on the surface. In the adsorption events nearly all of the  $\text{CH}_3$  energy is transferred to the substrate rather quickly, as the gas molecule reacts and forms a bond with one of the surface radical sites. We found a greater degree of surface carbon atom displacements if a larger amount of energy is transferred to the film. For a  $\text{CH}_3$  having an energy of more than 1 eV, we observed surface H release events involving the creation of new adsorption sites. We also found no evidence for induced surface damage even at the highest energies, suggesting that experiments with low or intermediate energy molecular beams might indeed yield high quality materials.

#### ACKNOWLEDGMENTS

We are grateful to D. W. Brenner for providing the spline routines that describe the parameters in his potential and we thank him, D. Ingram, M. Kordesch, and H. Richardson for fruitful discussions. We acknowledge support from the Ohio Supercomputer Center through project PHS060.

- <sup>1</sup>J.C. Angus and C.C. Hayman, *Science* **241**, 913 (1988); W.A. Yarbrough and R. Messier, *ibid.* **247**, 688 (1990); M. Cappelli and P.H. Paul, *J. Appl. Phys.* **67**, 2596 (1990); B.E. Williams, J.T. Glass, R.F. Davis, and K. Kobashi, *J. Cryst. Growth* **99**, 1168 (1990).
- <sup>2</sup>(a) L.R. Martin and W.H. Hill, *J. Mater. Sci. Lett.* **9**, 621 (1990); (b) N. Ohtake and M. Yoshikawa, *J. Electrochem. Soc.* **137**, 717 (1990); (c) P.J. Martin, S.W. Filipczuk, R.P. Netterfield, J.S. Field, D.S. Whitnall, and D.R. McKenzie, *J. Mater. Sci. Lett.* **7**, 410 (1988); (d) A.S. Bakai and V.E. Strel'nitskii [*Sov. Phys. Tech. Fiz.* **26**, 1425 (1981)].
- <sup>3</sup>F. Davanloo, E.M. Juengermann, D.R. Hander, T.J. Lee, and C.B. Collins, *J. Appl. Phys.* **67**, 2081 (1990).
- <sup>4</sup>(a) T. Miyazawa, S. Miyazawa, S. Yoshida, and S. Gonda, *J. Appl. Phys.* **55**, 188 (1984); (b) A. Anttila, J. Koskinen, R. Lappalainen, J.P. Hirvonen, D. Stone, and C. Paszkiet, *Appl. Phys. Lett.* **50**, 132 (1987); (c) J. Ishikawa, Y. Takeiri, K. Ogawa, and T. Takagi, *J. Appl. Phys.* **61**, 2509 (1987).
- <sup>5</sup>J.W. Zou, K. Schmidt, K. Reichelt, and B. Dischler, *J. Appl. Phys.* **68**, 1558 (1990).
- <sup>6</sup>R. Berman, *Physical Properties of Diamond* (Oxford University Press, London, 1965).
- <sup>7</sup>*Diamond and Diamond-Like Films and Coatings*, edited by R.E. Clausing, L.L. Hostou, J.C. Angus, and P. Koidl (Plenum, New York, 1991).
- <sup>8</sup>H.-P. Kaukonen and R.M. Nieminen, *Phys. Rev. Lett.* **68**, 620 (1992).
- <sup>9</sup>D.R. McKenzie, D. Muller, and B.A. Pailthorpe, *Phys. Rev. Lett.* **67**, 773 (1991).
- <sup>10</sup>M.H. Loh and M.A. Cappelli, *Diamond Relat. Mater.* **2**, 454 (1993); M.E. Kordesch (private communication).
- <sup>11</sup>S.J. Harris, *Appl. Phys. Lett.* **56**, 2298 (1990).
- <sup>12</sup>S.J. Harris and L.R. Martin, *J. Mater. Res.* **5**, 2313 (1990).
- <sup>13</sup>B.J. Garrison, E.J. Dawnkaski, D. Srivastava, and D.W. Brenner, *Science* **255**, 835 (1992).
- <sup>14</sup>D.W. Brenner (private communication).
- <sup>15</sup>D.W. Brenner, *Phys. Rev. B* **42**, 9458 (1990).
- <sup>16</sup>J. Tersoff, *Phys. Rev. Lett.* **56**, 632 (1986); *Phys. Rev. B* **37**, 6991 (1988).
- <sup>17</sup>H.J.C. Berendsen, J.P.M. Postma, W.F. van Gurensen, A. Dinola, and J.R. Haak, *J. Chem. Phys.* **81**, 8364 (1984).
- <sup>18</sup>L. Verlet, *Phys. Rev.* **159**, 98 (1967); D.W. Heerman, *Computer Simulation Methods in Theoretical Physics* (Springer, Berlin, 1986).